Check for updates

Performance Study of Aluminium–Zinc Anode using Noise Resistance, Pitting Index and Recurrence Plots from Electrochemical Noise Data

Nosa Idusuyi[1] · Ojo Sunday Fayomi[2]

Abstract

Electrochemical noise technique allows the simultaneous measurement of voltage and current on a material in a process stream. Useful information regarding the state of the sample, initiation, type and growth of corrosion can be obtained. To this end, time domain and recurrence plots have been used to study the electrochemical noise data obtained for an Al–Zn sacrificial anode immersed in NaCl solution over 7 days to understand various corrosion mechanisms occurring on the anode surface. The noise resistance, pitting index and recurrence plots were correlated with scanning electron microscopy (SEM). The results revealed that PI and R_n for the non-heat-treated and heat-treated aluminium–zinc anodes decreased progressively with immersion time. This can be attributed to increasing dissolution activity on the anode surfaces. The obtained R_n for non-heat-treated anodes were greater than $10^5 \, \Omega \, cm^2$ and the R_n for heat-treated anodes were less than $10^5 \, \Omega \, cm^2$. Heat treating the Al–Zn anodes helped to reduce the noise resistance values to a maximum of $12,000 \, \Omega \, cm^2$. The recurrence plots showed distinct butterfly-like structures that indicated progressive dissolution activity on the anode surfaces. Lower noise resistance and pitting index as immersion time progressed signified improved electrochemical performance of the anodes.

Keywords Electrochemical noise · Corrosion · Noise resistance · Pitting index · Recurrence plots

1 Introduction

Aluminium has been around for centuries, but gained prominence in the last 50 years as a material of choice for sacrificial anodes in the protection of pipelines for transporting petroleum products. Aluminium also finds extensive usage in building storage tanks, concrete structures, bridges, aerospace and military hardware, engine components, ship hulls and platforms [1–3]. It's preference has been mainly due to its low density, relative availability, excellent thermal properties, low specific weight, reasonable cost and a relatively high theoretical capacity of about 2980 Ahr/kg [2, 4]. Obtaining real-time information on the state of sacrificial anodes mounted on bridge structures is extremely needful to monitor and avoid the onset of corrosion which can result in failures and high fatalities. Several electrochemical techniques such as Potentiodynamic polarization, electrochemical impedance spectroscopy, weight loss method, electrochemical noise, and so on have been used to gain useful insights into the corrosion behaviour of aluminium anodes and other alloys in service [4–7]. Of all the techniques highlighted, electrochemical noise (ECN) presents unique advantages of been able to acquire mechanistic information about corrosion processes and types (uniform, localized or mixed) [8–10] during in situ monitoring of pipes with hard-to-reach areas [11], coatings [12], alloys for aerospace applications and composites [13–16], which may be difficult to obtain by other electrochemical techniques [17, 18]. It is a straightforward technique that does not require complex instrumentation like other measurement techniques and could be easily adapted for remote monitoring. However, the noise resistance and pitting index obtained from ECN can sometimes be unreliable and misleading in classifying the types of corrosion. To this end, several approaches have been used to further analyse ECN data such as statistical [12, 19], chaos [20, 21], wavelet analysis [15, 19, 22–25], recurrence plots and quantification analysis [26]. Recurrence plots (RP) are graphical techniques for nonlinear data analysis which is capable

✉ Nosa Idusuyi
  nosaidus@gmail.com

  Ojo Sunday Fayomi
  ojosundayfayomi3@gmail.com

1 Department of Mechanical Engineering, University of Ibadan, P.M.B. 5116, Ibadan, Oyo State, Nigeria

2 Department of Mechanical Engineering, Covenant University, P.M.B. 1023, Ota, Nigeria

of revealing specific times when the phase space trajectory of the dynamical system visits roughly the same area in the phase space [24, 26]. This technique can be used for any time series since it requires no previous knowledge of the statistical properties of the series. The method of recurrence plots (RP) was first introduced by Eckmann et al. [27] to visualize the dynamics of phase space trajectories. The present paper demonstrates the analysis of ECN data using statistical and recurrence plots to study typical corrosion data for a sacrificial anode system and to find out hidden patterns, understand surface activities and classify the possible types of corrosion occurring on the anodes.

2 Experimental

2.1 Specimen Preparation

An aluminium anode (Al–2.5 wt% Zn) was produced from pure aluminium and zinc ($> 99.75\%$) and used for the study. The chemical composition of the alloy was confirmed from optical emission spectroscopy (OES) shown in Table 1. The cut anode samples were heat treated at 150 °C for 1 h in a muffle furnace and subsequently quenched in water.

2.2 Electrochemical Noise Measurements

ECN measurements were performed using a typical electrochemical cell consisting of two working Al–Zn electrodes and a silver/silver chloride reference electrode on an Ivium CompactStat Potentiostat controlled with a custom Ivium software. Insulated wires were attached to the working electrodes of identical areas (1.768 cm^2) and covered with epoxy resin such that only one face of each sample was exposed. The surfaces were wet ground with 1000 grade SiC paper, washed thoroughly with distilled water and cleaned with acetone prior to testing. The test environment was 3 wt% NaCl buffered to pH 8 ± 0.3 using 0.5 M NaOH. All solutions were prepared from deionised water and analytical grade reagents. During ECN measurements, care was taken to ensure that the distance between all electrodes was consistent in each test. The tests were performed over a seven-day period beginning as the electrodes were immersed in the electrolyte. The current between the two working electrodes and the potential between the working electrodes and the reference electrode were simultaneously recorded at a frequency of 1 Hz (i.e., 1 point per second) for 1024 s which required $2n$ data points, with n usually being 8, 9, or 10 (i.e., 256, 512, or 1024) at various immersion times (24 h intervals). The experimental procedure is represented in Fig. 1.

2.3 Electrochemical Noise Analysis

2.3.1 Time Domain Analysis

The raw voltage and current (V–I) signals were measured with a total of 1024 data points and a linear trend subtracted (to take care of potential and current drifts in the course of measurements) [10, 13]. The V–I signals were used to ascertain the onset and progression of localized corrosion on the surface of the Al–Zn anodes.

The noise resistance was evaluated in the time domain from ohms law using;

$$R_n = \frac{\sigma(v)}{\sigma(i)}, \tag{1}$$

where $\sigma(v)$ and $\sigma(i)$ are the standard deviations of potential and current fluctuations of the raw V–I values (*the R_n was calculated by averaging*).

2.3.2 Recurrence Plots

To understand the corrosion behaviour of the anode in the medium, the ECN (current) data were converted to a recurrence plot. In brief, a recurrence plot is a graphical representation of a square matrix, expressed as:

$$R_{ij} = H(\varepsilon - ||x_i - x_j||), \tag{2}$$

where R_{ij} is the (i, j)th point in the recurrence plot, ε is predefined threshold value, x_i, x_j is measured ECN values (current for our study) at times i and j, and $||.||$ is Euclidean distance between this pair of data points. $H(.)$ is Heaviside function. This returns the value of one if the distance between x_i and x_j lies within the threshold. Otherwise, it will return zero.

A MATLAB toolbox developed by Yang [28] was used to generate the recurrence plots.
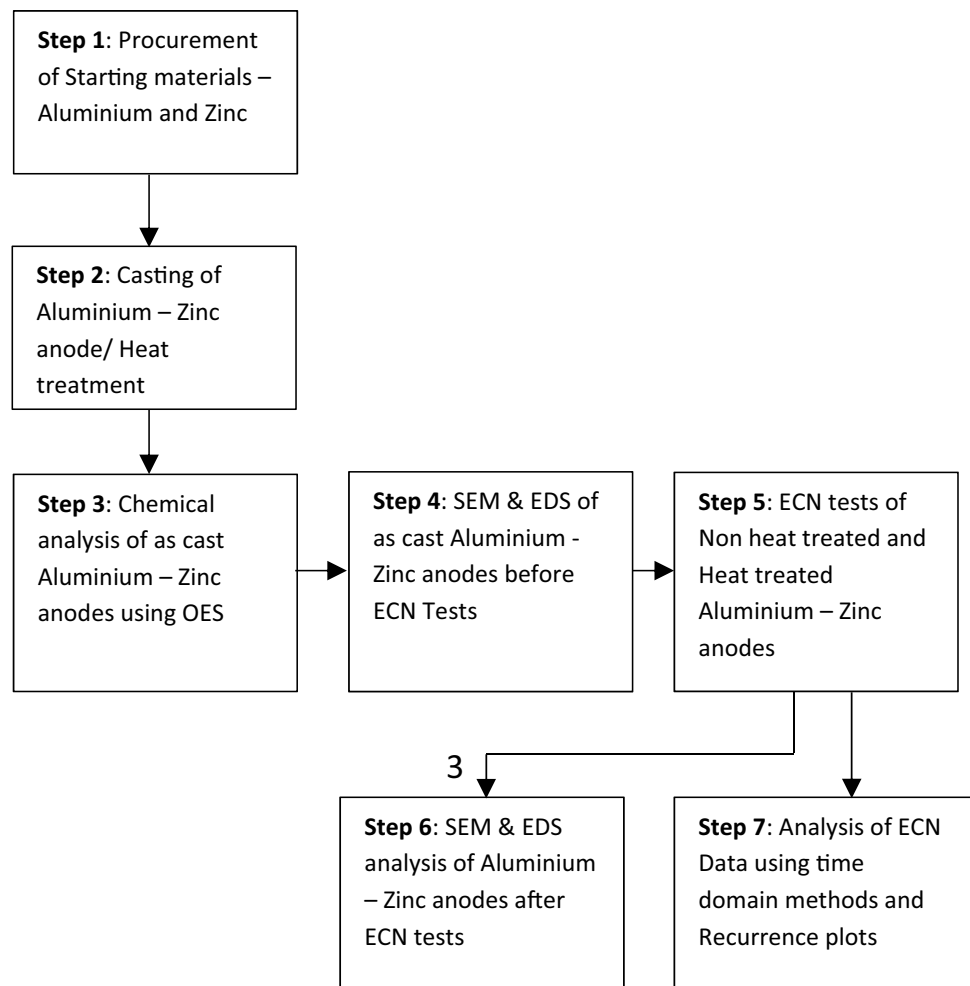
2.4 Metallographic Examination

The surfaces of the samples before and after ECN tests were examined using a scanning electron microscope (SEM, Tescan model) coupled with EDX, with an accelerating voltage of 20 kV, in the secondary electron mode.

Table 1 Chemical composition of Al–Zn anode used in the study

Element	Al	Zn	Si	Fe	Cu	Mn	Mg	Ti
%	97.01	2.52	0.068	0.101	0.012	0.0028	0.0014	0.0022

Other trace elements such as Ag, B, Be, Co, Li, Zr, and so on were present in very small percentages

Fig. 1 Experimental procedure

Step 1: Procurement of Starting materials – Aluminium and Zinc

Step 2: Casting of Aluminium – Zinc anode/ Heat treatment

Step 3: Chemical analysis of as cast Aluminium – Zinc anodes using OES

Step 4: SEM & EDS of as cast Aluminium - Zinc anodes before ECN Tests

Step 5: ECN tests of Non heat treated and Heat treated Aluminium – Zinc anodes

3

Step 6: SEM & EDS analysis of Aluminium – Zinc anodes after ECN tests

Step 7: Analysis of ECN Data using time domain methods and Recurrence plots

3 Results and Discussion

3.1 Electrochemical Noise Data for HT and NHT Anodes

The raw electrochemical noise data are shown in Fig. 2a–f. Section records of raw voltage and current signal plots for the non-heat-treated (NHT) and heat-treated (HT) samples at the start of the experiment (day 0), day 3 and 7 are shown. From the raw data plots, we observe that the potential and current noise exhibited high-frequency fluctuations especially at the start of immersion. The potential noise had peak values of 2.94 mV, 4.77 mV and 2.79 mV for the NHT anode; 3.09 mV, 8.27 mV and 2.94 mV for the HT anode. The corresponding peak current values were 0.06 nA, − 1.004 nA and 252.52 nA for the NHT anode; 7621.31 nA, 9426.08 nA and 1208.96 nA for the HT anode. The potential intensities were observed to drop consistently as immersion time progressed for NHT and HT, respectively. The current values were higher for the HT anodes for the duration of the experiment. However, there was a sharp

decline and then a gradual rise in the current values for HT anodes on the seventh day of immersion which could be attributed to formation of metastable pit. This behaviour has also been observed in a previous study by Ma et al. [29].

From Fig. 3a, the NHT anodes had average noise resistance (R_n) of 30.27×10^5, 13.07×10^5, 2.12×10^5 Ω cm^2 at the start, third and seventh day of immersion, respectively. Average R_n for the HT anodes was 1.2×10^3, 3×10^3 and 2×10^3 Ω cm^2 at the start, third and seventh day of immersion, respectively, as shown in Fig. 3b. This progressive decrease in noise resistance for the NHT anodes implied increasing dissolution activity on the anode surface as immersion time progressed. The significant drop (almost a 100% change) in the R_n for the HT anodes when compared to the NHT anodes indicates increased homogeneity in the alloy right from start of immersion. The R_n increased slightly probably due to the formation of a resistant thin film. Using a classification by Al-Mazeedi and Cottis [30], the obtained R_n for NHT anodes was greater than 10^5 Ω cm^2 indicating passivation especially for the first 72 h of immersion which improved as immersion time progressed.
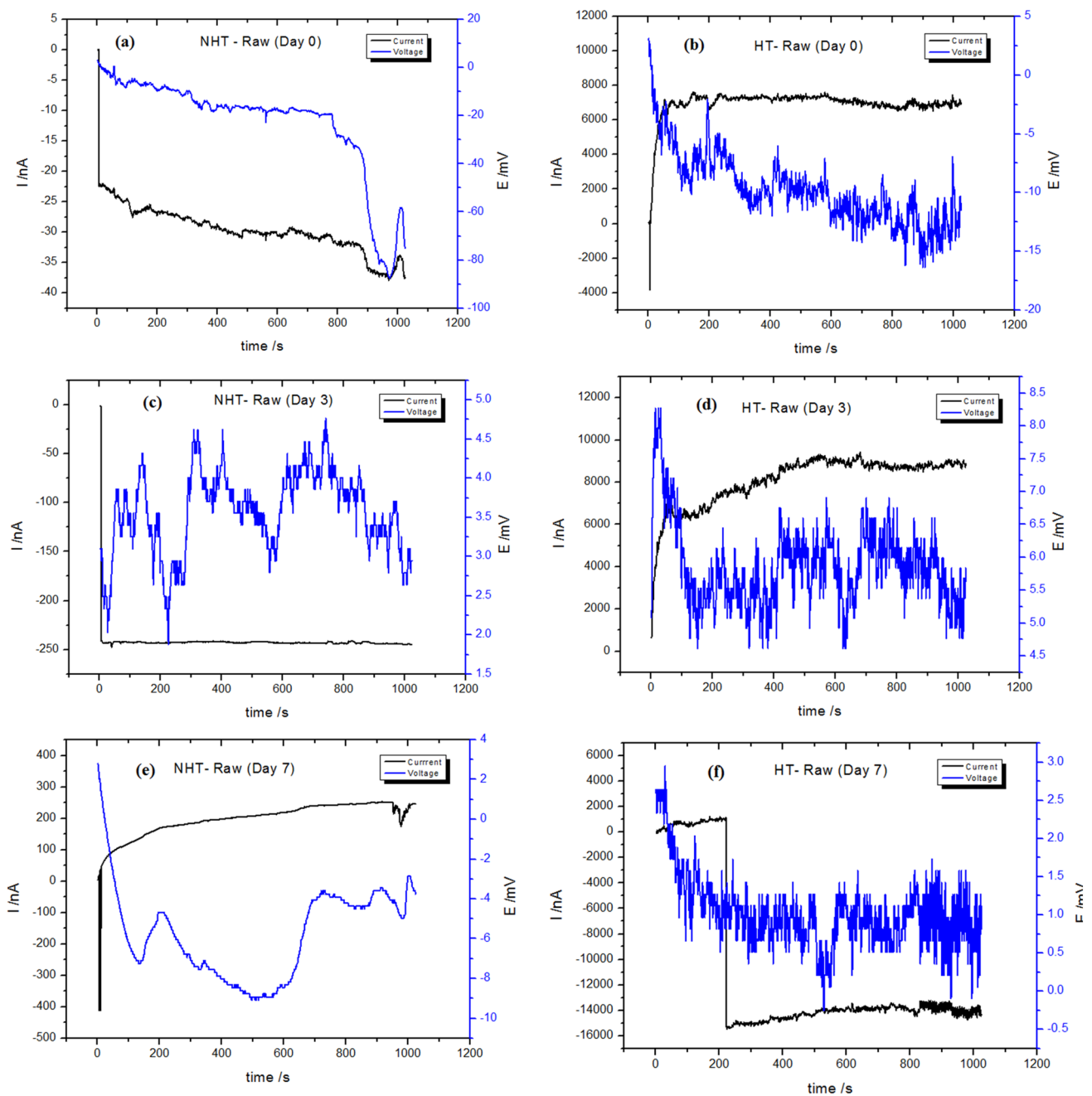
Fig. 2 **a–f** Raw potential–current values from ECN test

The R_n for HT anodes was less than 10^5 Ω cm^2 indicating uniform corrosion. The pitting or localization index (LI) for the Al–Zn anode was obtained from the acquired electrochemical noise data using an Ivium software. Figure 4 shows a combined plot of the pitting index (PI) versus time for the NHT and HT anode. Average PI of 0.0018, 0.00028 and 0.0021 was obtained at day 0, day 3 and day 7, respectively, for the NHT anodes. The average PI for the HT anodes was 0.0032, 0.0031 and 0.0029 at day 0, day

3 and day 7, respectively. The NHT anodes experienced a decrease between day 0 and day 3 and then an increase up till day 7. The HT anodes on the other hand showed a decreasing trend from the start to the end of the experiment. Using Eden and Rothwel's classification [31], the average PI measured for the duration of the experiments was under 10^{-3} which indicated the system was predominantly uniform corrosion. Recurrence plots were used to further clarify the system behaviour.
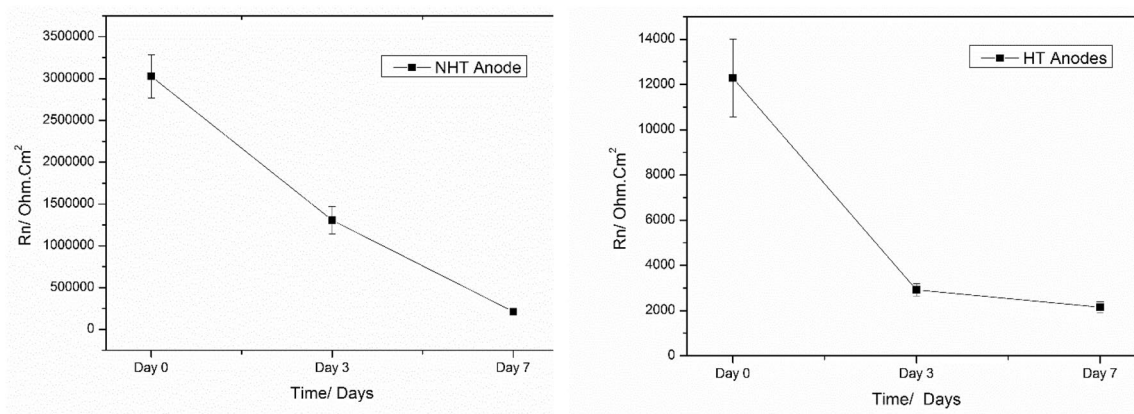
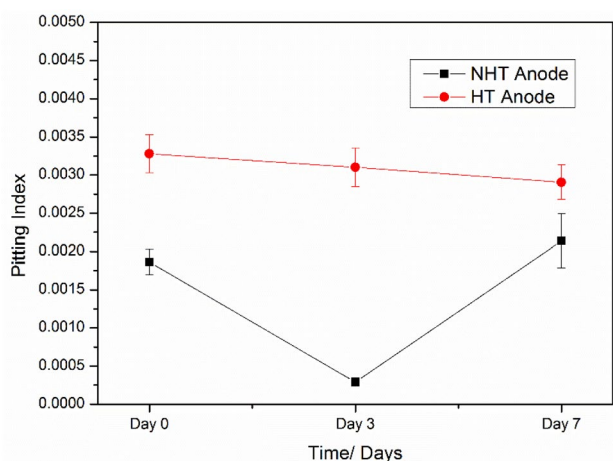**Fig. 3** **a** and **b** Average noise resistance for NHT and HT Al–Zn anode

Fig. 4 Average pitting index for NHT and HT Al–Zn anode

3.2 Recurrence Plots (RPs) of HT and NHT Anodes

To understand how the non-heat-treated (NHT) and heat-treated (HT) anode behave in the solution, raw electrochemical current data were first divided into short segments. Each of the segments had 1024 data points, which was equivalent to a time frame of 512 s. After removing the linear trend of each measured current segment, recurrence plots were generated by applying a threshold of 0.5 to the distance matrices. Information about the dynamics of a time series is obtained from the line structure and point density on RPs. A homogeneous RP with no structure is typical of a stationary process such as white noise. RPs of oscillating systems have diagonal lines or checkerboard patterns. Vertical or horizontal lines in a RP signify the presence of laminarity or intermittency in the time series, whereas abrupt changes in dynamics as well as extreme events are characterized by white areas or bands [32]. The RPs show visually the changes in the dynamics of the system as immersion time

progressed especially as the anode (NHT and HT) undergo dissolution, activation and passivation. The recurrence plots on Fig. 5a–f for day 0, 3 and 7 measured at 48 h intervals are presented here. The vertical and diagonal structures in the RPs from the NHT anodes display a decrease as immersion time progresses signifying a breakdown of the passivity on the anode surfaces. The presence of butterfly-like structures along the main diagonal (bisector) on the NHT anodes was an indication of dissolution activity. In this case, the start and end of an active dissolution correspond to the start and end of the formation of butterfly-like structure along the main diagonal. This butterfly pattern disappears towards the topmost edge. By day 7, the RP showed a predominantly linear structure indicating that the anodic dissolution activity tended towards been more stable and uniform. RPs for the HT anodes displayed a somewhat different trend as there was increased activity especially on day 3 (resembling a Brownian type motion) which could signal intense dissolution activities. This intense activity seemed to have disappeared by day 7 implying uniform corrosion activity. These results were in agreement with the noise resistance and pitting index obtained earlier.

3.3 Microstructural Study

Figure 6a–c shows the distribution of elements in the Al–Zn alloy prior to immersion and after ECN measurement. Fe appears as an impurity in the alloy with very low percentages. The EDS analysis of selected points on the surface revealed zinc depletion (point 1) on exposed surface and zinc rich areas (point 2) as the surfaces opened up during dissolution. From Table 2, high Oxygen percentages at point 1 also shows the accumulation of salt/water. Figure 7a–c shows signs of active dissolution on both surfaces of the electrode pair after the ECN tests.

Figure 8a, b shows evidence of pitting on the NHT and HT anode surfaces at lower magnifications. The pitting on
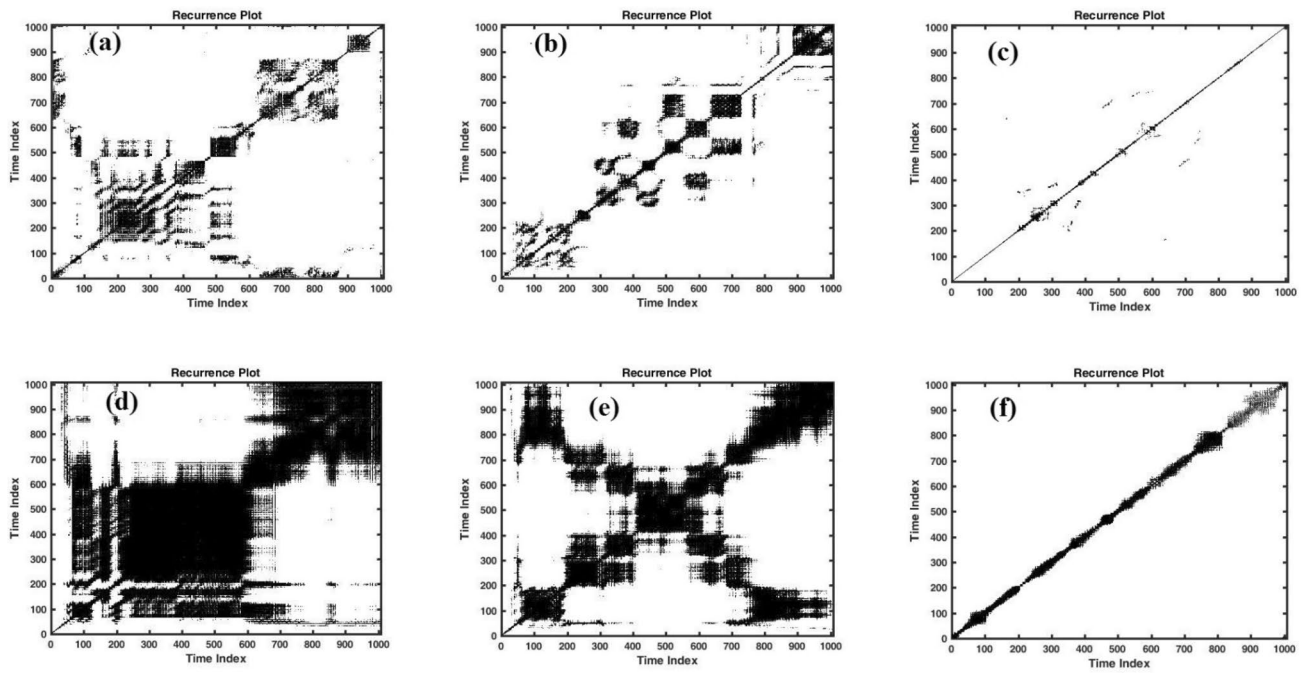
Fig. 5 Recurrence plots–NHT anodes (**a**–**c**) and HT anodes (**d**–**f**)
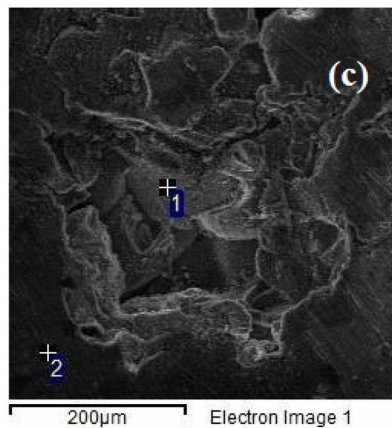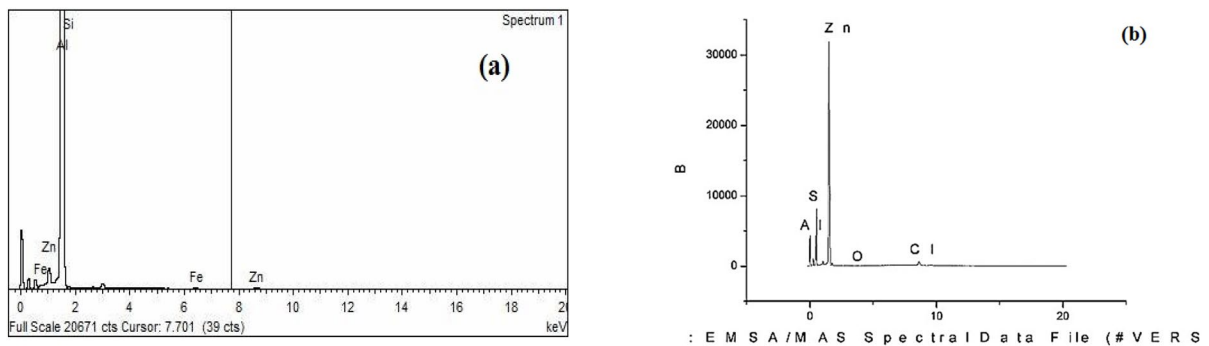
Fig. 6 **a** EDS before ECN test, **b** EDS after ECN test, and **c** EDS points after immersion test

Table 2 Elemental composition at points 1 and 2 for EDS after immersion

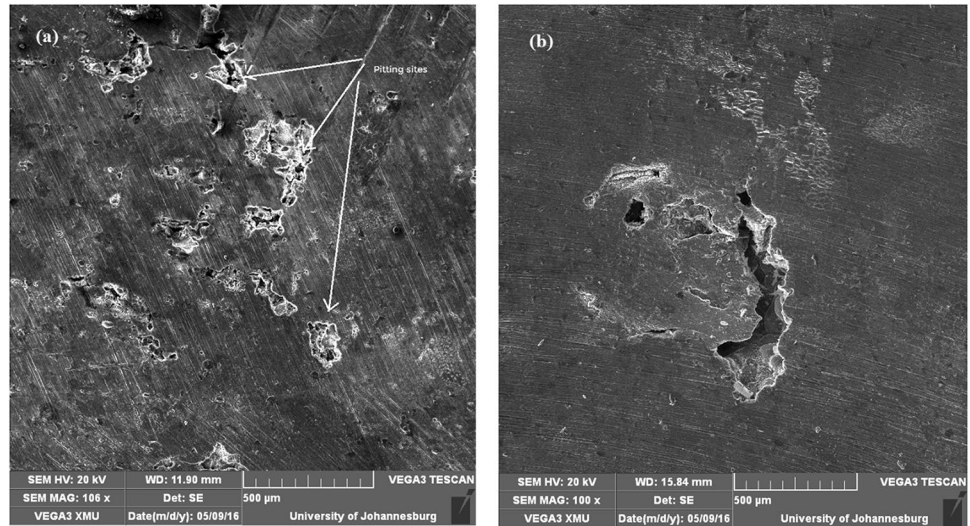| Spectrum	In stats	O	Al	Si	P	Cl	Zn	Ag	Total
1	Yes	40.02	49.22	0.89		0.11	9.76		100
2	Yes	18.69	75.07	0.55	0.13		2.07	3.48	100
Max		40.02	75.07	0.89	0.13	0.11	9.76	3.48	
Min		18.69	49.22	0.55	0.13	0.11	2.07	3.48	
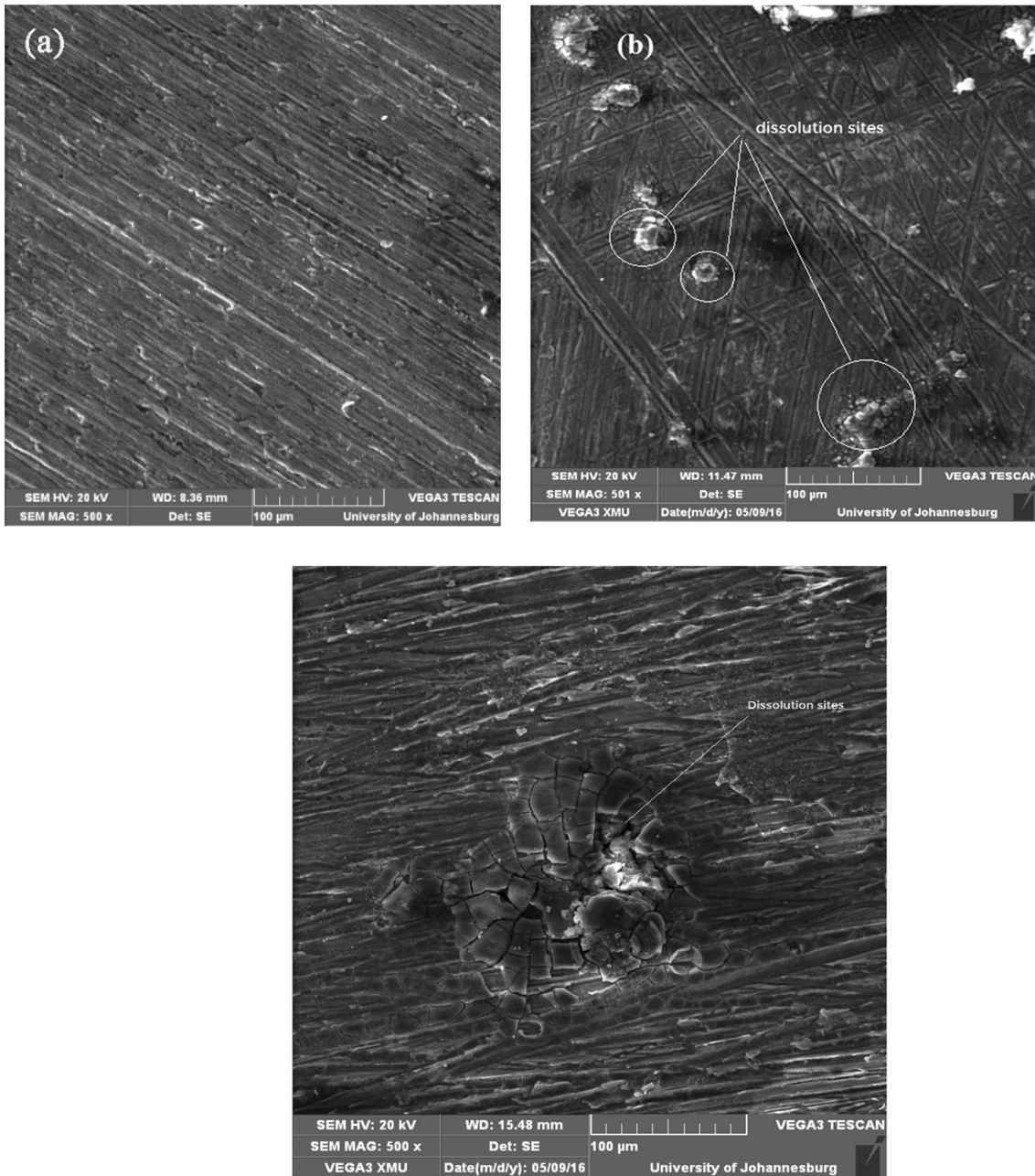
Fig. 7 **a** SEM for Al–Zn anode before ECN test, **b** SEM for NHT anode after ECN test and **c** SEM for HT anode after ECN test

Fig. 8 a SEM for NHT anode after ECN test (×100) and **b** SEM for HT anode after ECN test (×100)

the NHT anode surfaces appears to be more severe and spread out more on the surface of the anodes. But on close examination using Image J software, we find that the pits on the NHT anodes measured 100–250 μm on the average, compared to the HT anodes where the pits measured as much as 600 μm. These wide variation could possibly be the reasons for the intense fluctuations observed from ECN tests.

The pitting action on the anode surfaces can be explained using the reactions occurring on the surfaces. Briefly, the uniform corrosion of aluminium enables the formation of an Al_2O_3 passive film according to the following reaction:

$$2Al + 3H_2O \rightarrow Al_2O_3 + 6H^+ + 6e^-. \tag{3}$$
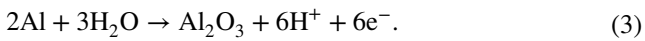
The Al_2O_3 film is not stable in water hence it becomes $Al(OH)_3$ by hydration [33]. The oxide layer film is generally porous and allows Cl^- ions penetration where local breakdown of the passive film gives initiation of pits. This penetrations enables the formation of $AlCl_3$ compound. On the other hand, the solubility of Zn in the aluminium matrix would result in the formation of Zn/Al galvanic cells on the anode surface [34]. However, zinc passivation will occur due to the formation of $Zn(OH)_2$ and ZnO passive films. However, in the presence of sodium chloride, these film becomes porous by chloride penetration and forms zinc hydroxide chloride $Zn_5(OH)_8Cl_2.H_2O$ [34]. A detailed schematic of the pitting process is presented in Fig. 9.

3.4 Future Work

This present paper demonstrates the ability to analyse corrosion data obtained from electrochemical noise experiments using statistical and recurrence plots for a sacrificial anode system. The incorporation of machine learning and fractal analysis will be explored in future studies to gain deeper insights into complex processes such as pit initiation and growth occurring on the anode surfaces.

Fig. 9 Schematic for pitting on Al–Zn anode surface
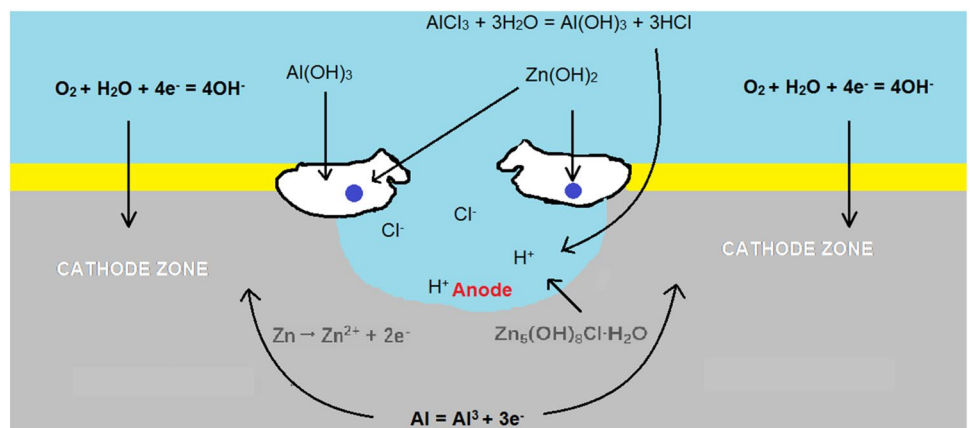
4 Conclusions

In this paper, we have studied the behaviour of a non-heat-treated and heat-treated Al–Zn anode using ECN data obtained from corrosion studies. Time domain and recurrence quantification were used to analyse the ECN data. From the results obtained, the following conclusions can be made:

- Noise resistance (R_n), pitting index (PI) and recurrence plots (RPs) can prove useful in identifying the onset of corrosion and dissolution activity on a sacrificial anode.
- Heat treating the Al–Zn anodes helped reduce the noise resistance values obtained from ECN technique. A maximum of 12,000 Ω cm^2 was obtained.
- The recurrence plots showed distinct butterfly-like structures that indicated progressive dissolution activity on the anode surfaces
- Scanning electron microscopy revealed dissolution activity on the anode surfaces.

Compliance with Ethical Standards

Conflict of interest On behalf of all authors, the corresponding author states that there is no conflict of interest.

References

1. Khajuria A, Akhtar M, Pandey Manish K, Singh Mayur P, Raina A, Bedi R, Singh B (2019) Influence of ceramic Al$_2$O$_3$ particulates on performance measures and surface characteristics during sinker EDM of stir cast AMMCs. World J Eng 16:526–538. https://doi.org/10.1108/WJE-01-2019-0015
2. Shibli SMA, Gireesh VS (2005) Activation of aluminium alloy sacrificial anodes by selenium. Corros Sci 47:2091–2097
3. Khajuria A, Bedi R, Singh B, Akhtar M (2018) EDM machinability and parametric optimisation of 2014Al/Al$_2$O$_3$ composite by RSM. Int J Mach Mach Mater 20:536. https://doi.org/10.1504/IJMMM.2018.096380
4. Oluwole OO, Idusuyi N (2012) Aluminium anode activation research—a review. Int J Sci Technol 2:561–566
5. Juárez-Islas J, i Llongueras JG (2000) Development and testing of galvanic anodes for cathodic protection. Contrib Sci 331–343
6. Talavera M, Valdez S, Juarez-Islas J, Mena B (2002) EIS testing of new aluminium sacrificial anodes. J Appl. http://link.springer.com/article. Accessed 7 Feb 2017
7. Idusuyi N, Ajide OO, Oluwole OO, Arotiba OA (2017) Electrochemical impedance study of an Al6063–12% SiC–Cr composite immersed in 3 wt% sodium chloride. Procedia Manuf 7:413–419. https://doi.org/10.1016/j.promfg.2016.12.019
8. Cottis RA (2001) Interpretation of electrochemical noise data. Corrosion 57:265–285
9. Hai D, Behnamian Y (2015) Electrochemical noise: a review of experimental setup, instrumentation and DC removal. Russ J Electrochem 51:593–601. https://doi.org/10.1134/S1023193515070071
10. Mansfeld F, Sun Z, Hsu CH (2001) Electrochemical noise analysis (ENA) for active and passive systems in chloride media. Electrochim Acta 46:3651–3664
11. Caines S, Khan F, Shirokoff J, Qiu W (2017) Demonstration of increased corrosion activity for insulated pipe systems using a simplified electrochemical potential noise method. J Loss Prev Process Ind 47:189–202. https://doi.org/10.1016/j.jlp.2017.03.012
12. Ashassi-Sorkhabi H, Seifzadeh D, Raghibi-Boroujeni M (2016) Analysis of electrochemical noise data in both time and frequency domains to evaluate the effect of ZnO nanopowder addition on the corrosion protection performance of epoxy coatings. Arab J Chem 9:S1320–S1327. https://doi.org/10.1016/j.arabjc.2012.02.018
13. Casajús P, Winzer N (2015) Electrochemical noise analysis of the corrosion of high-purity Mg–Al alloys. Corros Sci 94:316–326
14. Chen A, Cao F, Liao X, Liu W, Zheng L, Zhang J, Cao C (2013) Study of pitting corrosion on mild steel during wet–dry cycles by electrochemical noise analysis based on chaos theory. Corros Sci 66:183–195. https://doi.org/10.1016/j.corsci.2012.09.017
15. Jamali SS, Mills DJ, Cottis RA, Lan TY (2016) Analysis of electrochemical noise measurement on an organically coated metal. Prog Org Coat 96:52–57. https://doi.org/10.1016/j.porgcoat.2016.01.017
16. Jamali SS, Zhao Y, Gao Z, Li H, Hee AC (2016) In situ evaluation of corrosion damage using non-destructive electrochemical measurements—a case study. J Ind Eng Chem 43:36–43. https://doi.org/10.1016/j.jiec.2016.07.045
17. Liu XF, Zhan J, Liu QJ (2009) The influence of tensile stress on electrochemical noise from aluminum alloy in chloride media. Corros Sci 51:1460–1466. https://doi.org/10.1016/j.corsci.2009.03.035
18. Xia D-H, Ma C, Song S, Ma L, Wang J, Gao Z, Zhong C, Hu W (2017) Assessing atmospheric corrosion of metals by a novel electrochemical sensor combining with a thin insulating net using electrochemical noise technique. Sens Actuators B 252:353–358. https://doi.org/10.1016/j.snb.2017.05.179
19. Homborg AM, Cottis RA, Mol JMC (2016) An integrated approach in the time, frequency and time-frequency domain for the identification of corrosion using electrochemical noise. Electrochim Acta 222:627–640. https://doi.org/10.1016/j.electacta.2016.11.018
20. Mahjani MG, Moshrefi R, Sharifi-Viand A, Taherzad A, Jafarian M, Hasanlou F, Hosseini M (2016) Surface investigation by electrochemical methods and application of chaos theory and fractal geometry. Chaos Solitons Fractals 91:598–603. https://doi.org/10.1016/j.chaos.2016.08.011
21. Stringer J, Markworth AJ (1993) Applications of deterministic chaos theory to corrosion. Corros Sci 35:751–760. https://doi.org/10.1016/0010-938X(93)90212-Y
22. Homborg AM, Van Westing EPM, Tinga T, Zhang X, Oonincx PJ, Ferrari GM, De Wit JHW, Mol JMC (2013) Novel time–frequency characterization of electrochemical noise data in corrosion studies using Hilbert spectra Reference electrode. Corros Sci 66:97–110. https://doi.org/10.1016/j.corsci.2012.09.007
23. Huang JY, Guo XP, Qiu YB, Chen ZY (2007) Cluster and discriminant analysis of electrochemical noise data. Electrochim Acta 53:680–687. https://doi.org/10.1016/j.electacta.2007.07.058
24. Liu W, Wang D, Chen X, Wang C, Liu H (2017) Recurrence plot-based dynamic analysis on electrochemical noise of the evolutive corrosion process. Corros Sci 124:93–102. https://doi.org/10.1016/j.corsci.2017.05.012

25. Moshrefi R, Mahjani MG, Jafarian M (2014) Application of wavelet entropy in analysis of electrochemical noise for corrosion type identification. Electrochem Commun 48:49–51. https://doi.org/10.1016/j.elecom.2014.08.005

26. Hou Y, Aldrich C, Lepkova K, Machuca LL, Kinsella B (2017) Analysis of electrochemical noise data by use of recurrence quantification analysis and machine learning methods. Int J Eng Sci Technol 256:337–347

27. Eckmann J-P, Kamphorst SO, Ruelle D (1987) Recurrence plots of dynamical systems. Europhys Lett 4:973–977. https://doi.org/10.1209/0295-5075/4/9/004

28. Yang H (2011) Multiscale recurrence quantification analysis of spatial vector cardiogram (VCG) signals. IEEE Trans Biomed Eng 58:339–347

29. Ma J, Wen J, Li Q (2013) Electrochemical noise analysis of the corrosion behaviors of Al–Zn–In based alloy in NaCl solution. Phys Procedia 50:421–426. https://doi.org/10.1016/j.phpro.2013.11.065

30. Al-Mazeedi HAA, Cottis RA (2004) A practical evaluation of electrochemical noise parameters as indicators of corrosion type.

31. Electrochim Acta 49:2787–2793. https://doi.org/10.1016/j.electacta.2004.01.040

31. Eden DA, Rothwell AN (1992) Electrochemical noise data: analysis, interpretation and presentation. Corrosion/92, Paper No. 292

32. Marwan N (2003) Encounters with neighbours: current development of concepts based on recurrence plots and their applications. University at Potsdam, Potsdam

33. Okeoma KB, Owate IO, Oguzie EE, Mejeha IM (2012) Impacts of heat treatment on the electrochemical properties of AA3003 expose to 0.1 M hydrochloric acid media. Am J Mater Sci 2:51–58. https://doi.org/10.5923/j.materials.20120201.10

34. Khireche S, Boughrara D, Kadri A, Hamadou L, Benbrahim N (2014) Corrosion mechanism of Al, Al–Zn and Al–Zn–Sn alloys in 3 wt% NaCl solution. Corros Sci 87:504–516